

DELIVERABLE REPORT



NEXUS

Evaporated PVSK top cell with abundant materials, bandgap in the range 1.65-1.75 eV, PCE (>20%) passing T95 stability tests.

Deliverable D1.2
September-2025

PREPARED BY
PARTNER UVEG
COORDINATED BY
CEA

Grant Agreement n°101075330

NEXUS is a 3-year research and innovation project funded by the European Commission through the Horizon Europe Research and Innovation Action (RIA) grant N°101075330, responding to the call for a “Sustainable, secure and competitive energy supply” (HORIZON-CL5-2021-D3-02).

NEXUS aims to accelerate Europe’s energy transition by developing perovskite-silicon tandem photovoltaic technology, via a new European paradigm: an eco-design approach, based on efficiency, cost, sustainability, circularity and social aspects and using abundant materials. NEXUS aims to develop stable, 2-terminal perovskite-silicon tandem solar cells and modules with high power conversion efficiencies, using sustainable, coherent and competitive European PV production, to create a viable economic pathway for the European commercialisation of this technology.

NEXUS is formed of a multi-disciplinary consortium: 13 partners from 10 countries; 6 industrial partners & 7 RTOs, covering the whole value chain of innovation from research centres to technology providers, end-users and market and policies.

Project info	101075330 – NEXUS – HORIZON-CL5-2021-D3-02-04
Deliverable Title	D1.2: Evaporated PVSK top cell with abundant materials, bandgap in the range 1.65-1.75 eV, PCE (>20%) passing t95 stability tests.
Lead Beneficiary	UVEG
Authors	Sam Teale, Paul Fassel, Maximiliano Senno, Lidon Gil-Escrig, Jorge Ferrando, Henry J. Snaith and Henk J. Bolink
Approved by	Henry J. Snaith
Dissemination level	Public
Due date	30/4/2025
Submission date	30/9/2025
Version	V3
Linked to WP - task	WP1 – T1.1 Development of high-performance evaporated perovskite thin films of suitable bandgap

Legal notice

This document only reflects the authors' view, and the Union is not liable for any use that may be made of the information contained therein.

© This document is the property of the NEXUS Consortium. This document may not be copied, reproduced, or modified in whole or in part for any purpose without written permission from the NEXUS Consortium, which consists of the following participants:

NEXUS Consortium

Organization name	Short name	Country
COMMISSARIAT A L'ENERGIE ATOMIQUE ET AUX ENERGIES ALTERNATIVES	CEA	FR
ACCADEMIA EUROPEA DI BOLZANO	EURAC	IT
KARLSRUHER INSTITUT FUER TECHNOLOGIE	KIT	DE
RIJKSUNIVERSITEIT GRONINGEN	RUG	NL
SALD B.V	SALD	NL
UNIVERSITAT DE VALENCIA	UVEG	ES
3 SUN S.R.L.	3SUN	IT
ICARES CONSULTING	BI	BE
NORSUN AS	NORSUN	NO
THE CHANCELLOR, MASTERS AND SCHOLARS OF THE UNIVERSITY OF OXFORD	UOXF	UK
OXFORD PHOTOVOLTAICS LIMITED	OPV	UK
FACHHOCHSCHULE NORDWESTSCHWEIZ	FHNW	CH
ODTU GUNES ENERJISI UYGULAMA VE ARA STIRMA MERKEZI	GUNAM	TR



© Members of the NEXUS Consortium

Disclaimer

Funded by the European Union. Views and opinions expressed are however those of the author(s) only and do not necessarily reflect those of the European Union or CINEA. Neither the European Union nor the granting authority can be held responsible for them.

How to Cite

Sam Teale, Paul Fassel, Maximiliano Senno, Lidon Gil-Escrig, Jorge Ferrando, Henry J. Snaith and Henk J. Bolink (2025). Deliverable 1.2 Report: Evaporated PVS_K top cell with abundant materials, bandgap in the range 1.65-1.75 eV, PCE (>20%) passing t95 stability tests. in Project NEXUS: Next Generation of Sustainable Perovskite-Silicon Tandem Cells (No. 101075330). European Union. PUBLIC [Communicate on 30/09/2025].

Table of Content

Table of Content.....	4
1. Executive Summary	5
1.1. Description of the deliverable content and purpose	5
1.2. Relation with other activities in the project.....	5
2. Results	6
2.1. Power conversion efficiency (PCE)	6
2.2. Stability.....	8
2.2.1. Difficulties in measuring cell temperature during accelerated aging	8
2.2.2. Temperature and bias dependent aging (UOXF).....	14
2.2.3. Stability summary from other NEXUS partners:.....	19
3. Conclusions.....	23

1. Executive Summary

Using a perovskite consisting of Cesium Formamidium Lead Iodide Bromide (CsFAPbI₃Br) with a bandgap around 1.68 eV, we prepared single junction solar cells that have maximum power point tracked power conversion efficiencies in the range of 18 to 20.3 %. Three methods were used to prepare the perovskite: a) by co-sublimation of all its precursors or b) by co-sublimation of the inorganic precursors followed by the addition of the organic precursors in a benign solvent via the so-called “hybrid method” and c) by sequential evaporation, whereby the inorganic components are evaporated in a first step, followed by the organic-halide salt in a second step.

To ensure correct reporting, significant effort has been expended to ensure that the reported aging temperature used herein is the actual temperature of a perovskite solar cell while aging in the study. Notably this revealed that previous aging temperatures reported by UOXF were considerably higher than the actual cell temperature. Hence, we have formulated a new protocol that all NEXUS partners have adopted.

From this standpoint, we implemented a bias and temperature dependent aging study where we identified a strong dependence on the predicted outdoor stability of these cells in different locations ranging from 105 to 12.5 years in Oxford and Valencia, respectively, for the most stable cell architectures.

1.1. Description of the deliverable content and purpose

In this deliverable we evaluate the temperature and bias dependence of the performance of single junction perovskite solar cells over time. Importantly, the perovskite layer is prepared a) by co-sublimation of all its precursors (full vacuum method), b) by co-sublimation of the inorganic precursors followed by the addition of the organic precursors in a benign solvent (hybrid method), or c) by sequential sublimation of the inorganic precursors followed by the sublimation of the organic precursors (sequential evaporation method). Hence, in all cases no harmful or high boiling point solvents are used. The most stable of these single junction solar cells (bandgap of ~1.68 eV) reach power conversion efficiencies of up to 20% and have an estimated lifetime of 42 and 5.6 years, for Oxford (U.K.) and Valencia (Spain), respectively. These estimated lifetimes were derived from accelerated testing at different temperatures and cell conditions. Due to practical issues the highest temperature applied was not as high as initially intended. The stability of some of the cells, reaching \leq 5% degradation from the peak efficiency after 700 hours under illumination at 75 °C are significant as they suggest that these cells will be stable enough for first applications in northern to central European locations.

1.2. Relation with other activities in the project

The cell stability is related to most of the other work packages of the project.

2. Results

2.1. Power conversion efficiency (PCE)

A diagram of the solar cell configuration used is presented in Figure 1: Schematic of the cell layout used in this study., in which MeO-2PACz is (2-(3,6-Dimethoxy-9H-carbazol-9-yl)ethyl)phosphonic acid, which is used as the hole-transport layer (HTL), EDAI is ethylenediamoniumiodide used as a thermally evaporated passivation layer and BCP is bathocuproine. Fully vacuum processed and hybrid processed perovskite films were integrated into p-i-n “superstrate” single junction solar cells. In this configuration the (sun) light reaches the perovskite absorber via the glass substrate, a transparent conductive oxide (TCO) layer and an HTL. The electron transport layer (ETL) and a reflective metal electrode (Cu) are deposited on top of the perovskite. For the stability evaluation, aged under light and temperature in air, these cells were encapsulated using either a thin Al₂O₃ layer processed by atomic layer deposition at UVEG, or sputter coated SiO_x at UOXF, followed by glass lamination, such that on both sides of the solar cells, glass protects the cell from moisture and oxygen from the air. At KIT, the cells were not encapsulated but aged in a nitrogen atmosphere. The highest efficiency of these solar cells based on the full vacuum and hybrid processed perovskites are depicted in Figure 2 and Figure 3, respectively. The current-voltage curve derived power conversion efficiency (PCE) reaching 19.8% and 21.3%, respectively, with maximum power point (MPP)-tracked efficiencies of 19.2% and 20.3% respectively.

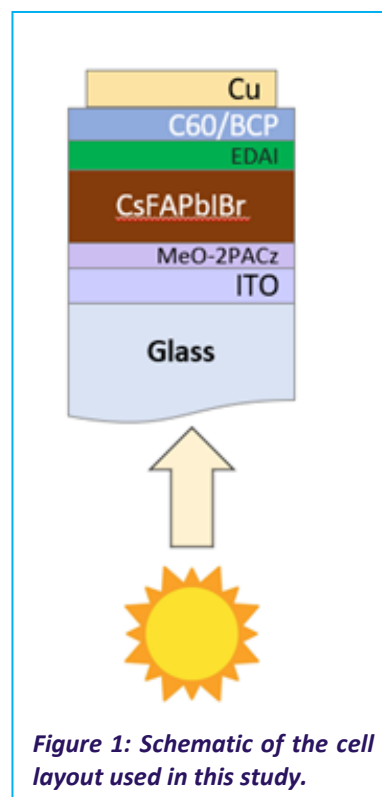


Figure 1: Schematic of the cell layout used in this study.

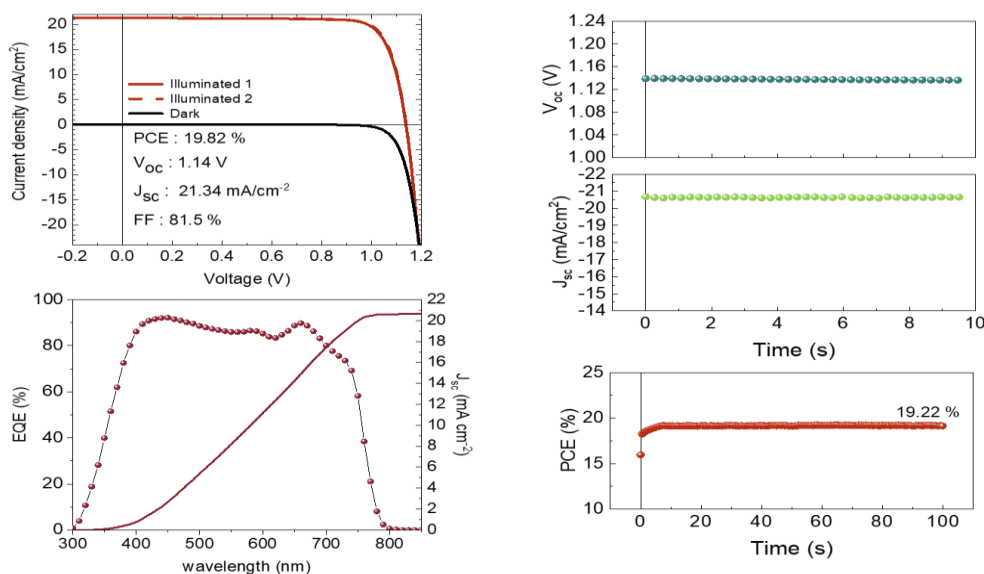


Figure 2: Initial performance of the solar cells employing the perovskite prepared by co-sublimation of all precursors. Panels show; current density (J) versus driving voltage (V) in the dark (black curve) and under AM1.5G simulated sunlight (“1 sun”) at 100 mW/cm² (inset shows the key performance parameters), external quantum efficiency (EQE) as a function of wavelength and integrated current density derived from it, Voltage,

Current density and power conversion efficiency (PCE) obtained from maximum power point (mpp) tracking.

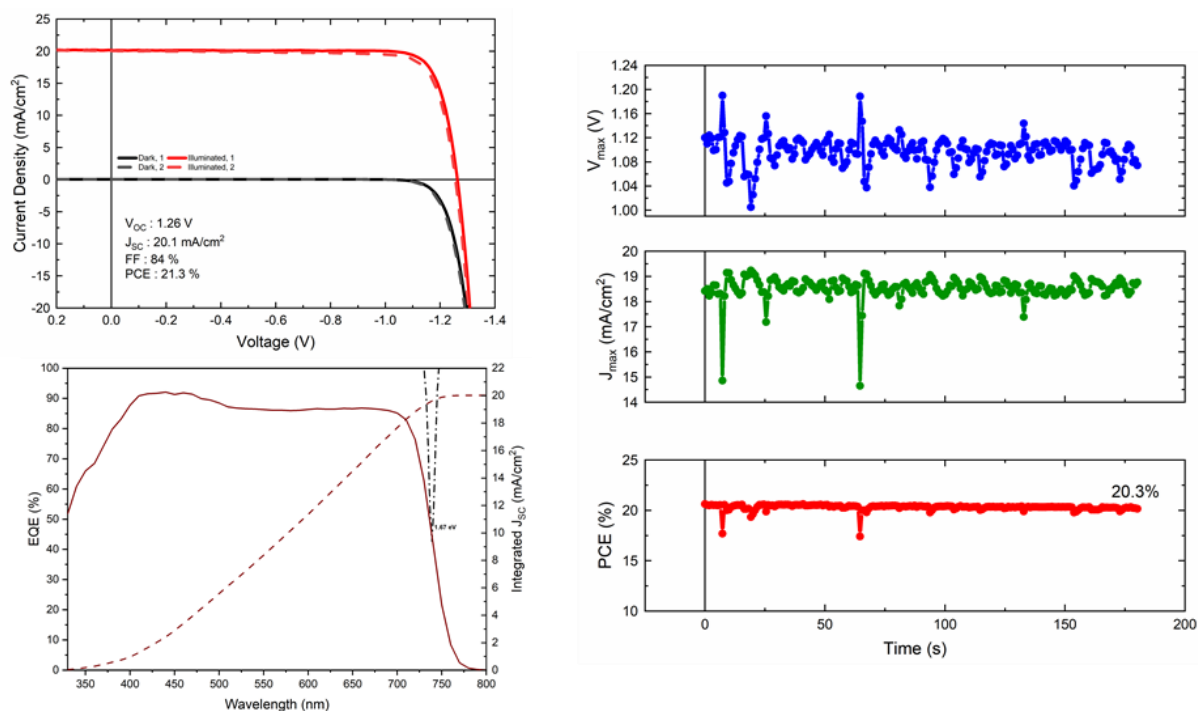


Figure 3: Initial performance of the solar cells employing the perovskite prepared with the hybrid method. Panels show; current density (J) versus driving voltage (V) in the dark (black curve) and under AM1.5G simulated sunlight (“1 sun”) at 100 mW/cm^2 (inset shows the key performance parameters), external quantum efficiency (EQE) as a function of wavelength and integrated current density derived from it, Voltage, Current density and power conversion efficiency (PCE) obtained from maximum power point (mpp) tracking

KIT prepared $\sim 1.68 \text{ eV}$ evaporated perovskite solar cells by (i) co-sublimation (composition $\text{Cs}_{0.2}\text{FA}_{0.8}\text{Pb}(\text{I}_{0.75}\text{Br}_{0.25})_3$) and (ii) sequential evaporation with the layer stack ITO/MeO-2PACz/perovskite/ C_{60} /SnO_x/Au. The perovskite film for sequential evaporation was formed by depositing CsCl/PbBr₂/PbI₂/FAI in sequence. The statistics of the J - V characteristics are shown in Figure 4. We note that no additional passivation was employed at the perovskite/ C_{60} interface. The champion pixels for both recipes achieve PCEs of 16.8% for co-deposition and 17.3% for sequential deposition (Figure 5).

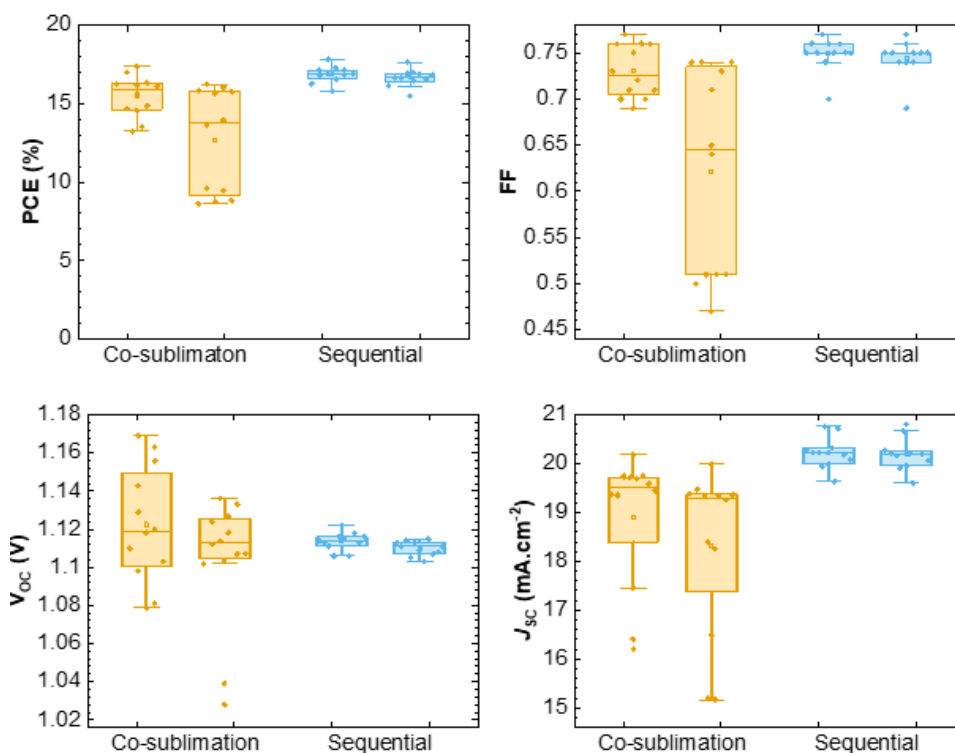


Figure 4: Performance comparison of perovskites solar cells fabricated via co-sublimation and sequentially evaporation with ~1.68 eV bandgap.

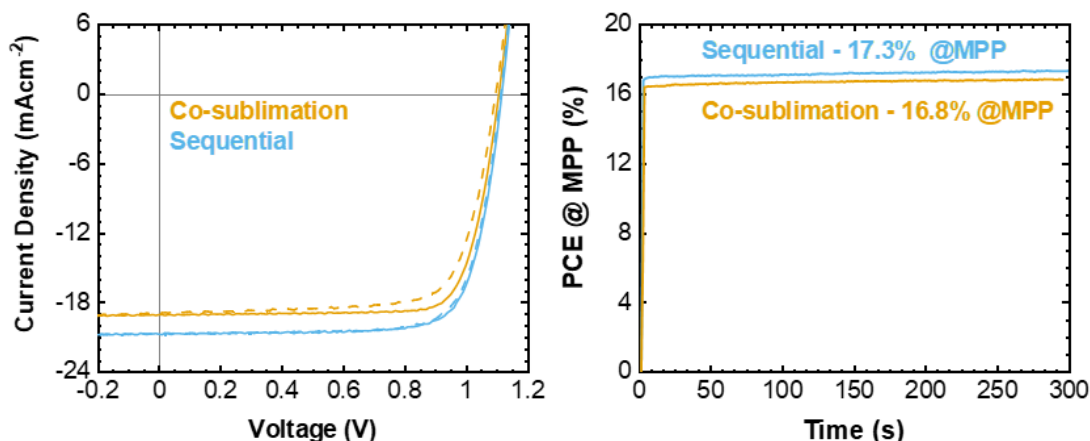


Figure 5: J-V characteristics (left) and stabilized power output (right) of champion pixels for co-sublimed and sequentially evaporated perovskite solar cells with ~1.68 eV bandgap.

2.2. Stability

2.2.1. Difficulties in measuring cell temperature during accelerated aging

A major challenge to the commercial viability for perovskite solar cells is proving their long-term operational stability in outdoor usage. Advances in composition and cell design have produced perovskite solar cells that show slow degradation after prolonged periods (months) in the field. Thus, researchers are turning to accelerated testing studies to quantify lifetimes. In these studies, cells are tested under harsher conditions than experienced outdoors, and this data is used to predict in-field lifetimes.

It is widely accepted that for perovskite solar cells under illumination, elevated temperature causes faster degradation. Unfortunately, most reported studies of stability neglect to describe in detail how the temperature of the aged device are derived, thus it is difficult to compare different studies between different laboratories. In order to translate laboratory measured degradation rates to real world predicted lifetimes, it is also essential to know as accurately as possible the cell temperature during aging and then to relate this to the estimated temperature the solar cell will experience when outdoors.

Indeed, there are inherent difficulties in assessing the temperature of a solar cell. First, directly measuring the temperature of each cell under aging is impractical and mechanically difficult when dealing with encapsulated cells. Thus, aging rigs typically contain a so-called “black standard” which is built from a non-degrading material containing a thermocouple for temperature regulation, that sits among the cells. Unfortunately, this leads to a second complication: under illumination heat is generated in the absorber layer, but the amount of heat generated depends on the type of solar cell in question. It can differ significantly from the black body standard since the solar cell will have different light absorption and reflection properties (e.g. wider-band gap materials will absorb less light than narrower band gap ones), different emissivity and the “packaging” of the cell will have different thermal conduction properties as compared with the black temperature standard. Furthermore, many aging setups use a fan to regulate the chamber temperate. This method of cooling can result in objects with lower thermal masses than the black standard (say a small, thin solar cell) being colder than the temperature measured on the standard.

2.2.1.1. Protocol developed at the UOXF

Aware of the issues mentioned above, we began our stability research in NEXUS by ensuring that we correctly measure the temperature of our cells during aging. We did this by fabricating a “cell-like” standard with similar thermal mass to a perovskite thin film solar cell. A black anodized piece of aluminium was bonded to a thermocouple and ITO/glass substrate using thermal epoxy (Figure 6). For each aging rig used in our testing, we compared the temperature of this new “cell-like standard” thermocouple to a thermocouple attached directly to the rear metal of a perovskite cell.

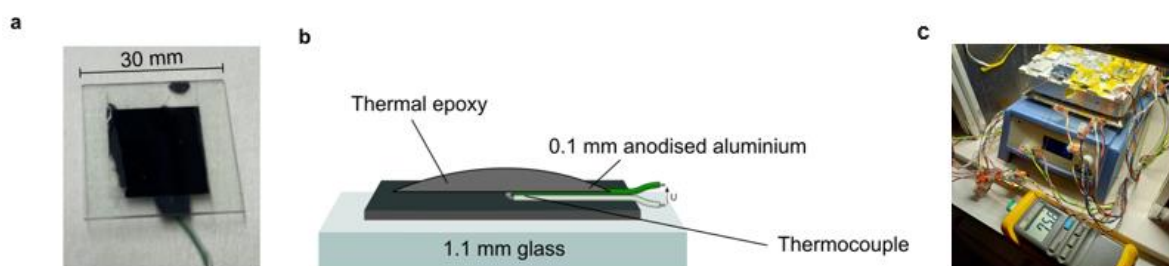


Figure 6: “Cell-like” standard. a) Picture of the cell-like standard. b) Diagram of the cell-like standard make up. c) Picture of the actual setup at UVEG.

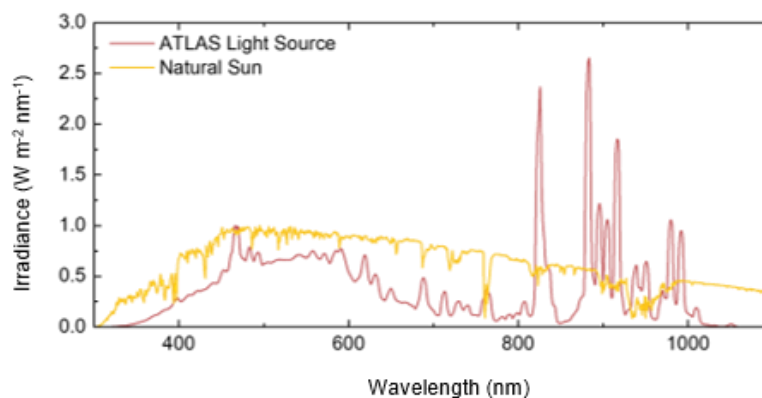


Figure 7: Spectrum of the Atlas box light source used to test the stability of solar cells in UOXF, compared to the AM1.5 spectrum (Natural Sun)

Initially, we assessed the cell temperature within an industry standard aging box (Atlas SUNTEST). These boxes contain a xenon bulb for illumination and heating under simulated full-spectrum sunlight with $\sim 77 \text{ mW cm}^{-2}$ irradiance (Figure 7). These have been regularly used by researchers at UOXF and others around the world to assess stability under illumination at elevated temperatures, under open-circuit conditions. The aging box used is heated via the lamp and air-cooled to control the temperature, which we set as $85 \text{ }^\circ\text{C}$, measured using an internal black standard positioned in the same plane and next to the test cells.

We used this aging rig to assess the stability of 1.67 eV fully evaporated solar cells prepared by UOXF under open-circuit conditions; the results are shown Figure 8. The median time it takes for the cells to drop to 80% of their starting efficiency (T80) of 18 cells was ~ 350 hours, whereas the T80 of the champion cell was 1000 hours. We considered this to be a good starting point as these cells were kept under open-circuit conditions. It is known that this condition leads to faster degradation than when the cells are maintained at their MPP-tracked efficiency (as used for operational cells).¹

However, on assessment of this aging rig using our “cell-like” black standard, we found that the temperature registered on the internal standard was considerably lower than the cell-like standard. Though the internal black standard registered $85 \text{ }^\circ\text{C}$, the small cell-like standard measured $65 \pm 5 \text{ }^\circ\text{C}$, suggesting that previous reports on stability at elevated temperature using this aging rig were not accurate. Notably, our target of a T95 of 1000 hours under $85 \text{ }^\circ\text{C}$ and simulated sun light, was based on where the state-of-the-art cell stability was at the time, when aged in this ATLAS aging box. Hence, we now know that $85 \text{ }^\circ\text{C}$ as measured by the black temperature standard in the atlas box actually corresponds to $65 \pm 5 \text{ }^\circ\text{C}$ in the cell. For the work reported here, we have altered the placement of the internal temperature standard so that it and the “cell-like” standard are at $80 \pm 5 \text{ }^\circ\text{C}$. Still this system is not fool-proof, as cells with wider bandgaps will necessarily absorb less light, meaning they do not heat as much as narrower gap cells. Hence, we moved to alternative dedicated light rigs, with the temperature assessed and controlled by “cell-like” black standards or thermocouples directly adhered to the rear of cells, to assess the performance of cells for this project.

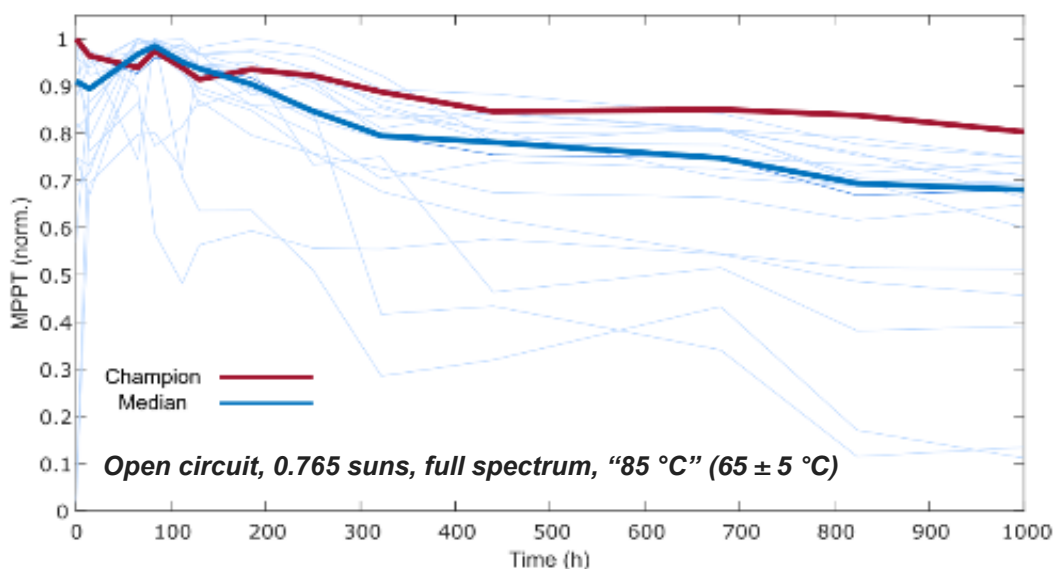


Figure 8: Stability curves for 18 fully evaporated perovskite solar cells (1.67 eV). The median (T80 = 350 hours) and champion cell (T80 ~ 1000 hours) are highlighted.

In this dedicated chamber, cells are continuously illuminated with 455 nm blue light at a 1-sun-equivalent intensity, defined as the photon flux required to generate a carrier density equivalent to that produced under the full solar spectrum at “1 sun” (AM1.5G 100 mW cm⁻²). To ensure that the LED irradiance source does not degrade, it is cooled via a connected water block. Heat to the sample is supplied via illumination with fans for blowing room temperature air through the chamber for cooling. In this rig, our cell-like standard was used for temperature regulation. By placing a thermocouple directly on the back electrode of a 1.67 eV perovskite cell, we compared the temperature of the cell-like standard and an actual solar cell. The results are shown in Figure 9 demonstrating that both are equivalent.

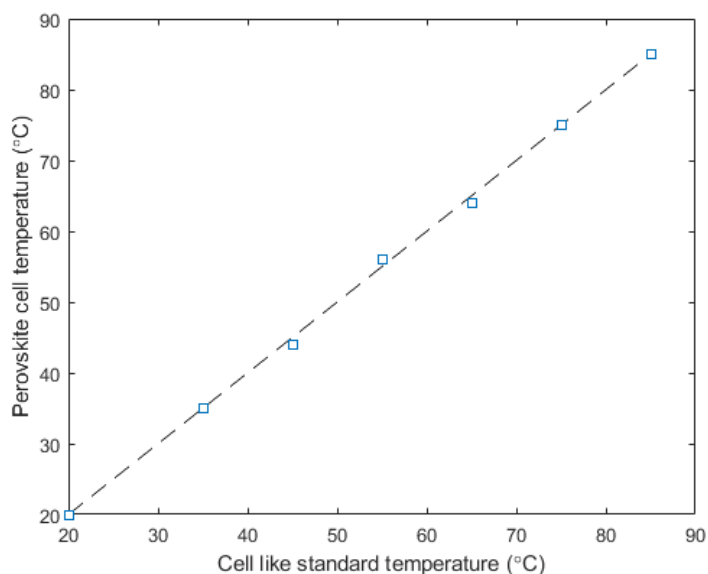


Figure 9: Comparison between the cell like standard's temperature and the perovskite cell temperature within

the dedicated aging rig (455 nm illumination).

Though measurement of temperatures up to 85 °C were obtained here, over a period of hours this warped the sample holders and damaged the electronics used for MPP tracking, and thus 85 °C stability data from this test set up does not feature in this report. A more robust tracking system is being implemented for future work.

2.2.1.2. Protocol developed at the University of Valencia (UVEG)

At UVEG, a type K thermocouple (naked junction) was encapsulated using the same protocol as the solar cells, employing Everlight AB-302 resin (transparent) tinted black to mimic the cell color. To further verify consistency, a second type K thermocouple was later encapsulated on a non-functional (“dummy”) perovskite solar cell using Everlight® AB-341 resin, yielding comparable results. All measurements were performed with an RS Pro 206-3722 digital thermometer, as illustrated in the accompanying figure and diagram (Figure 4c).

Regarding thermal stress, it was observed that maintaining a constant temperature of 85 °C caused the illumination LEDs to degrade over time. To mitigate this issue and keep the LEDs at a lower temperature at which they emit light stable over several months, a ventilator was added to the setup. This ventilator, however, lowered the maximum operating temperature of the solar cells to 75 °C.

The LED spectrum of the Kellwood Parker 3 series par3-100-750-110 (Led Philips Lumileds 3000) used in this setup is shown in Figure 10, and was measured using a spectrometer Ocean Optics Flame T series. The illumination power of the indoor setup was calibrated to match the short-circuit current obtained with the AAA solar simulator Wavelabs Sinus 70 Advanced before encapsulation.

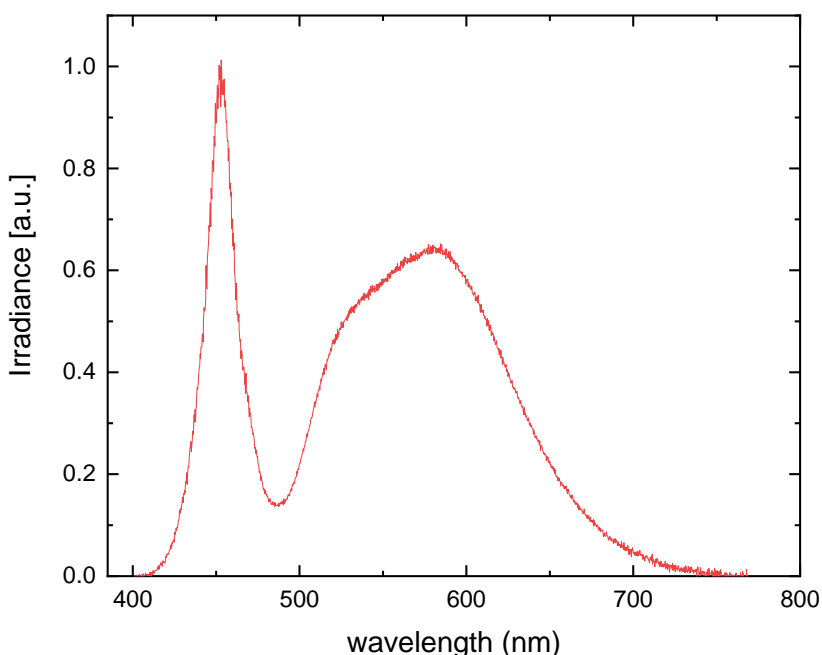


Figure 10: Normalized spectrums of Kelwood Parker 3 series (Built in LED: Philips Lumileds 3000) system, used to stress the devices

2.2.1.3. Protocol developed at Karlsruhe Institute of Technology (KIT)

The measurements at KIT were made in a glove box with N₂ atmosphere and equipped with a source meter (Keithley, 2400) and a Xenon lamp (Enlitech). The spectra of the light source is shown in Figure 11. The calibration of the lamp was performed using a certified Si reference solar cell (Fraunhofer) with KG5 filter (Schott). Sample holders with gold (Au) pins were used to contact the cells for electrical characterizations. We note that we observed that the sample holders (3D-printed from Polyvinyl Chloride in-house) slowly started to melt/decompose at temperatures of ~85° C which is why the maximum temperature of the setup was limited to ~80° C to allow long-term operation. The active area of the cell was 0.105 cm² and an aperture mask of 0.0784 cm² was used during characterization and aging. *J-V* characterizations were performed at a light intensity of 100 mW/cm² and a scan speed of 600 mV/s.

For MPP tracking, *J-V* characterization was performed first to identify the voltage at the maximum power point (V_m). Current was measured at this voltage. After a predetermined time interval, a small perturbation of $\pm V_{\text{perturb}}$ was applied around V_m and the current was measured again. Power outputs at V_m , $V_m + V_{\text{perturb}}$ and $V_m - V_{\text{perturb}}$ were compared. In the subsequent step, the tracking voltage was updated to the point among the three voltages where maximum power was observed. This process was repeated continuously, allowing the system to dynamically follow and maintain operation at MPP. A $\pm V_{\text{perturb}}$ of 10 mV was applied and the tracking interval was every 5 minutes.

The temperature of the cell was controlled at 80 °C employing a Peltier element, a PT100 temperature sensor and a microcontroller. The cell was placed on a holder with a copper (Cu) stage (see Figure 12). An electrically isolating, thermally conducting cloth was used to electrically isolate the Au contact from the Cu stage. The top and the bottom of the Cu stage has holes for the PT100 sensor, which was used to detect the temperature on the top and bottom of the copper stage and to control the current flow, depending on if the cell was to be maintained at 25 °C or 80 °C. Thermal glue was used to get good contact between the sensor and the Cu stage. A software is used to determine the temperature at the sample stage. While the temperature stabilizes, fluctuations of the temperature up to 83 °C were observed. The set temperatures were verified using a thermocouple on the substrate (glass side).

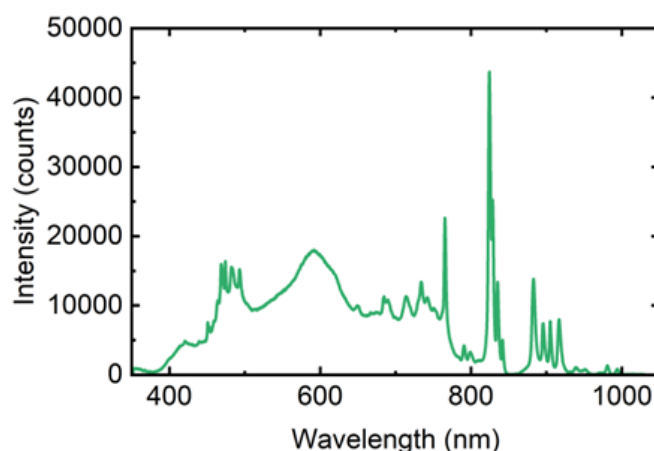


Figure 11: Spectrum of the Xenon lamp used for the J-V measurements and MPP tracking at KIT.

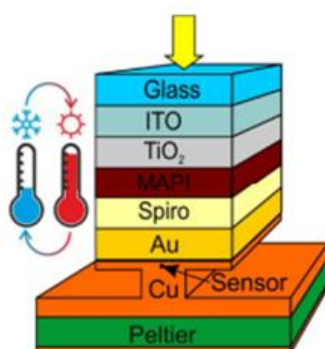


Figure 12: Temperature measurement and temperature control implemented during J-V characterization and MPP tracking at KIT. Reproduced from ACS Appl. Mater. Interfaces 2018, 10, 19, 16390–16399.

Finally, it should be noted that the experiences revealed above are not unique to this consortium. In fact, these issues (unreliable temperature measurements and poor equipment stability) are widespread. However, the NEXUS project has allowed significant discussion between labs on this subject, and we are planning to put this together as a perspective on proper measurements to age solar cells. This represents an important but unanticipated output of NEXUS.

2.2.2. Temperature and bias dependent aging (UOXF)

To ensure that the stability analysis used in this report is accurate, all experiments reported here were placed within the dedicated aging box at UOXF (455 nm, 1 sun illumination) where the temperature of the cells was matched to the “cell-like” standard, and monitored throughout the aging process as described in section 2.2.1. Only 1.67 eV perovskite solar cells for the NEXUS project were assessed in this chamber.

Rather than measuring only at one temperature and one bias condition (as in most studies), we were able to measure the cells at different aging temperatures (55, 65 and 75 °C) and under different bias conditions (open circuit, short circuit and MPP). Note that, as mentioned in section 2.2.1, an attempt to age at 85 °C damaged the sample holders and MPP tracking electronics and was hence not included in this study.

In commercial PV systems, solar cells operate at their MPP, but testing at this condition requires expensive electronics, limiting the number of cells that can be tested simultaneously. Tests at open-circuit conditions are simple, requiring no hardware other than a light source and the cell itself, allowing for larger sample sets. We measured a large sample set of devices (80 cells, tests shown in Table 1) and used this to statistically evaluate the difference in stability for each condition.

Cells were kept in the aging box at their set condition and regularly removed to test under our AM1.5 sunlight solar simulator. We monitored the changes in short-circuit current, open-circuit voltage, fill factor (FF) and MPP-tracked PCE over time. The results for each temperature are shown in Figure 13, Figure 14 and Figure 15.

Table 1: Conditions used for testing in the dedicated stability rig used to test (1.67 eV) NEXUS cells at UOXF.

Temperature (°C)	Illumination condition	Bias condition	Number of devices
55	1-sun-equivalent illumination using 455 nm blue light LED array	Open circuit	14
		Short circuit	6
		Maximum power point	5
65		Open circuit	13
		Short circuit	12
		Maximum power point	5
75		Open circuit	8
		Short circuit	12
		Maximum power point	5
Total number of devices:			80

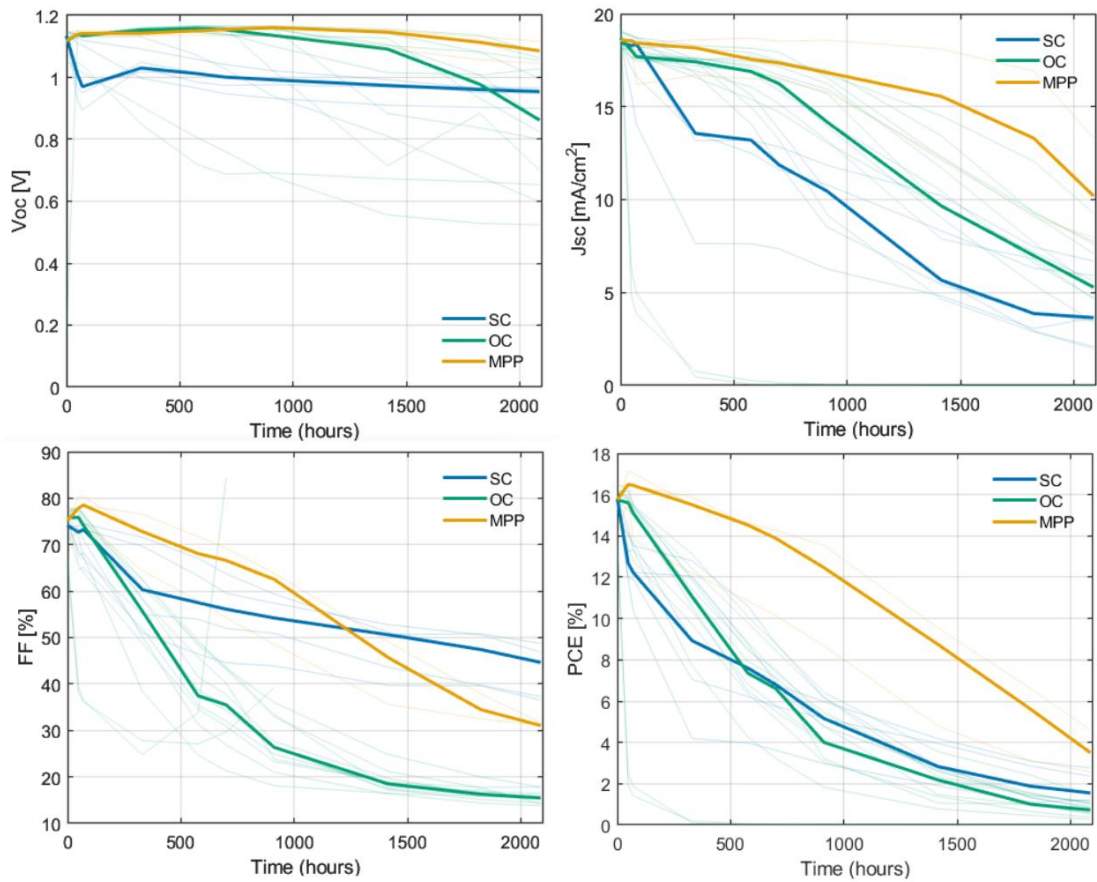


Figure 13: Stability curves tracking the performance of 1.67 eV evaporated perovskite solar cells under 1-sun-equivalent illumination (455 nm LEDs), at 55 °C under different bias conditions. The lighter coloured lines represent the performance of individual cells. The solid lines are the median of those.

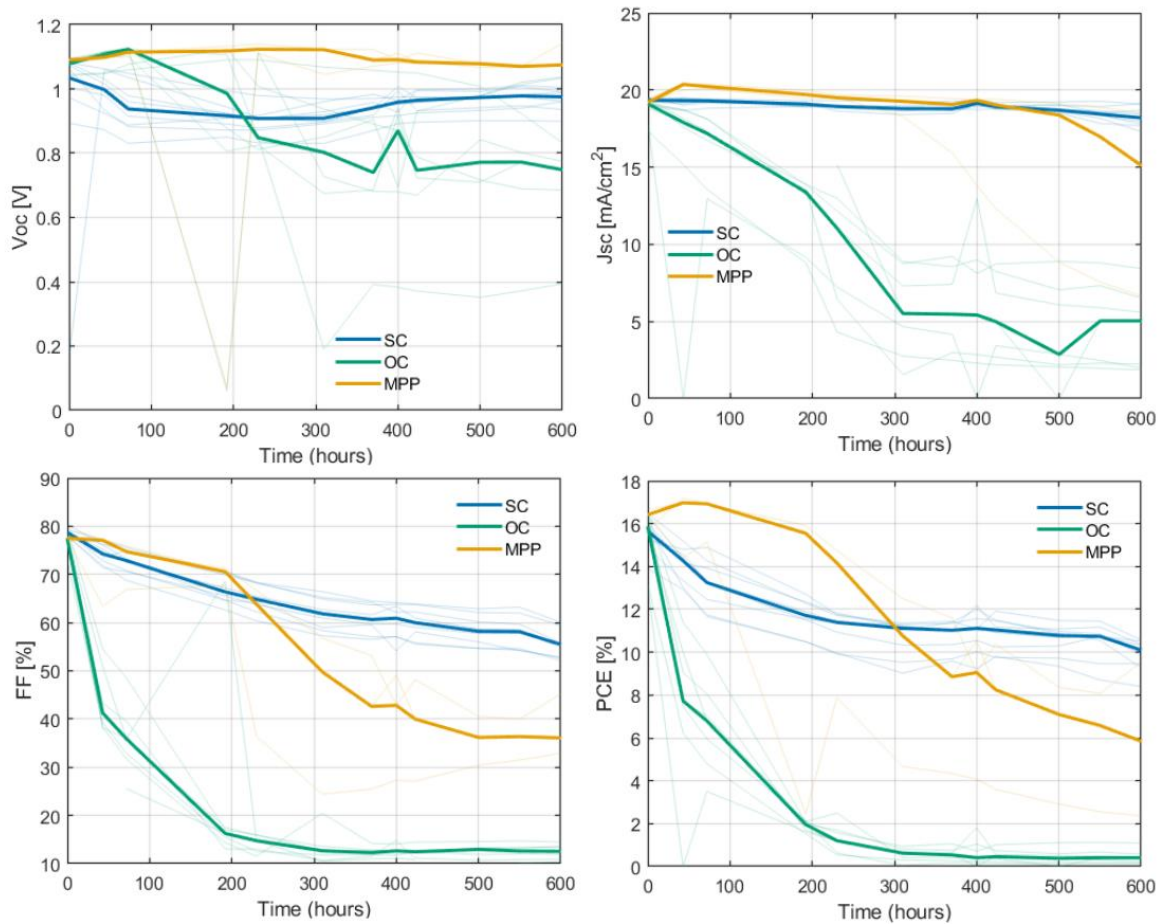


Figure 14: Stability curves tracking the performance of 1.67 eV evaporated perovskite solar cells under 1-sun-equivalent illumination (455 nm LEDs), at 65 °C under different bias conditions. The lighter coloured lines represent the performance of individual cells. The solid lines are the median of those.

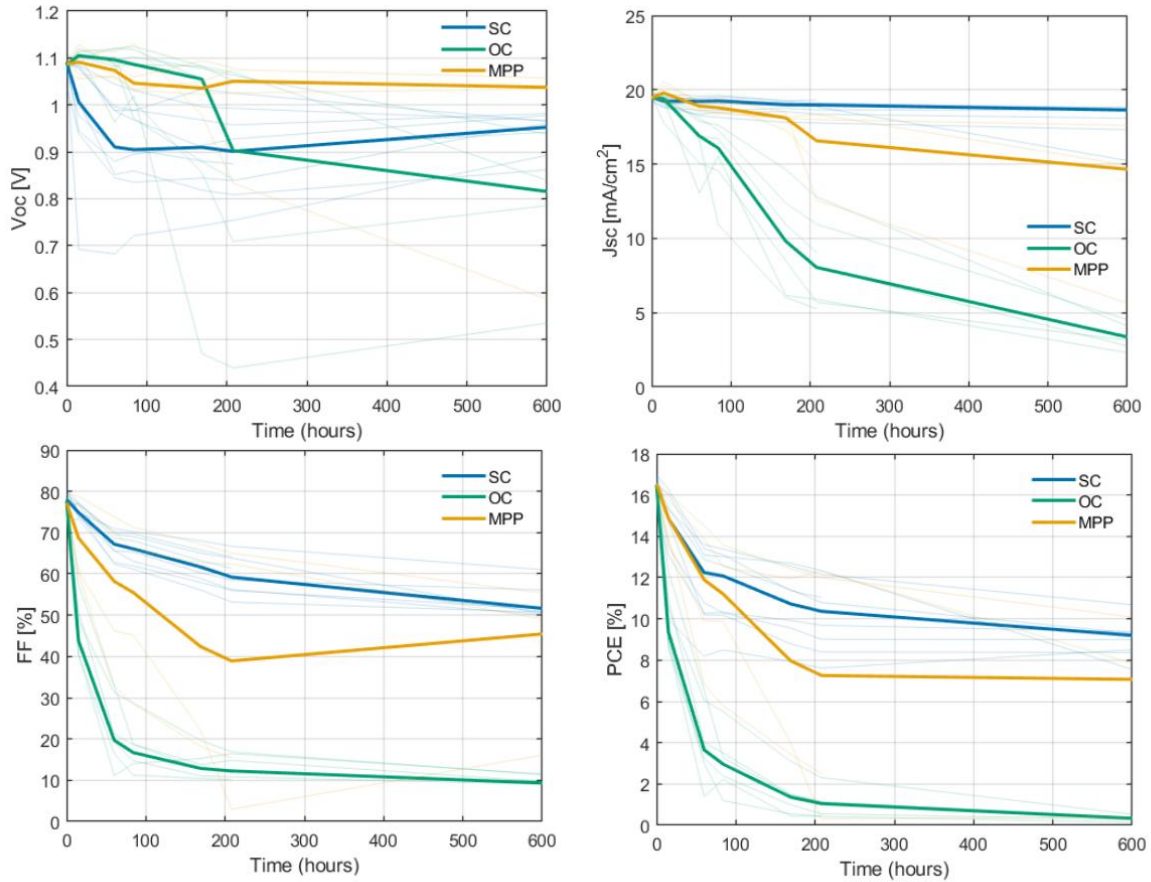


Figure 15: Stability curves tracking the performance of 1.67 eV evaporated perovskite solar cells under 1-sun-equivalent illumination (455 nm LEDs), at 75 °C under different bias conditions. The lighter coloured lines represent the performance of individual cells. The solid lines are the median of those.

We find a strong interdependence between cell stability, aging temperature and bias condition, meaning both need to be considered in any stability assessment. As our data is temperature dependent, we can use the Arrhenius relationship to extrapolate stability at different temperatures from this data. We fit our data to an exponential decay (as this fits better than a linear or biexponential decay) with decay constant k ,

$$PCE(t) = PCE(0)e^{-kt}$$

where t is the time in hours. We then fit this to the Arrhenius relationship

$$k(T) = A \exp\left(\frac{-E_a}{k_b T}\right)$$

where T is temperature in K, E_a is the activation energy of degradation, k_b is Boltzmann's constant, and A is a constant. By fitting k for each cell against temperature we can derive E_a , which we can use to estimate the stability of cells under the same illumination and bias conditions, but at a different temperature. Figure 16 plots k against $1/T$ and displays the calculated activation energies for each bias condition with associated uncertainty. Though the uncertainty bars are large, the relationship between each bias condition is clearly distinct, with essentially negligible change in degradation rate with temperature at short-circuit and temperature, and a very strong dependency between

degradation rate and temperature for open-circuit aging.

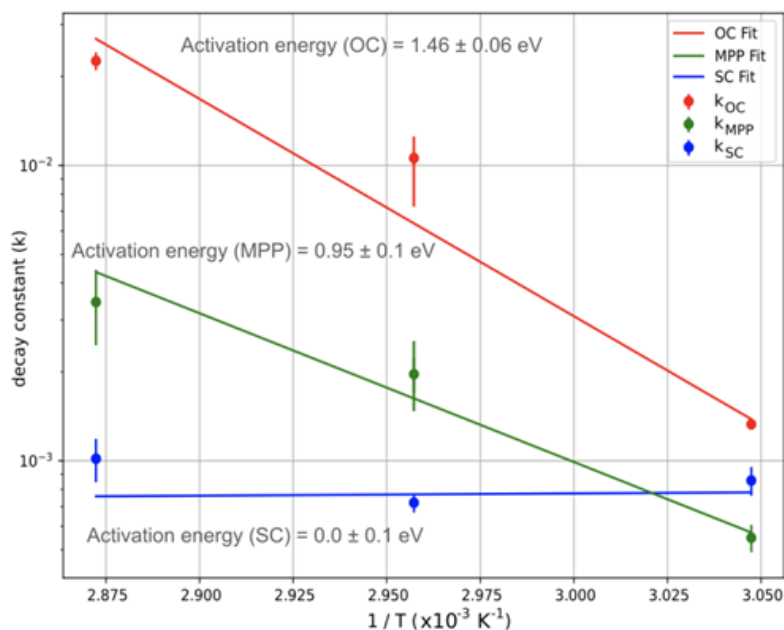


Figure 16: Decay constant against reciprocal temperature plot to derive activation energy of decay for each bias condition for 1.67 eV evaporated perovskite solar cells. Uncertainty bars represent the spread of decay data from device statistics.

Importantly, this demonstrates that aging cells at MPP is much less detrimental to performance than aging at open-circuit conditions for all temperatures in our study, with approximately ten-fold slower degradation under MPP than open circuit at 75°C. Hence, stability at MPP is used for further analysis. Notably, solar modules used outdoors will also be operated at MPP, making this the relevant condition for aging studies.

2.2.3. Stability summary from other NEXUS partners:

2.2.3.1. Devices measured at KIT

For stability assessment, representative devices – initial PCEs at 25 °C were 15.5% for co-sublimation and 16.6% for sequential evaporation – were stressed at 80 °C under 1-sun-equivalent illumination in a N₂-filled glovebox using a Xe lamp (Enlitech) without any additional encapsulation as described in section 2.2.1. The results are shown in Figure 17 and Figure 18 and yield T₈₀ of ~250 h for both recipes.

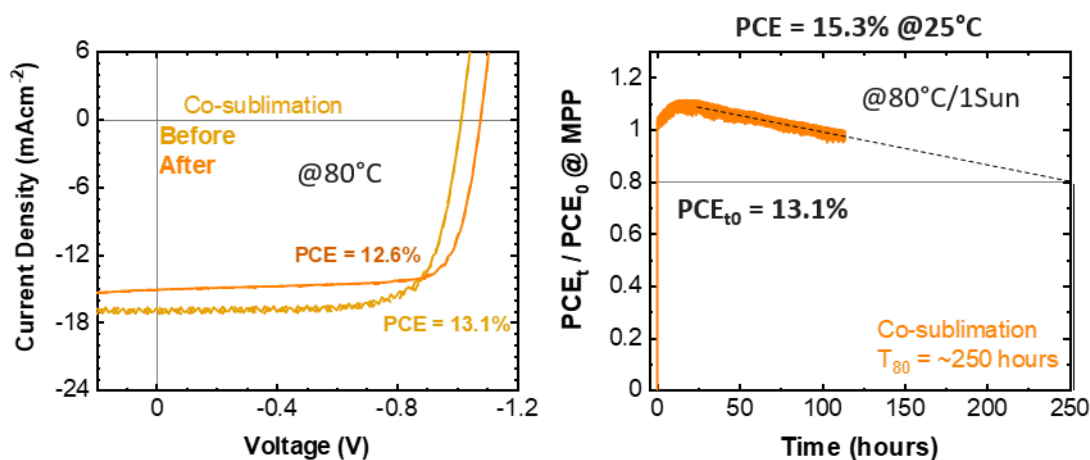


Figure 17: J-V characteristics before and after aging at 80°/1 sun (left) and MPP tracking with extrapolated T₈₀ (right) for a representative co-sublimed ~1.68 eV perovskite solar cell.

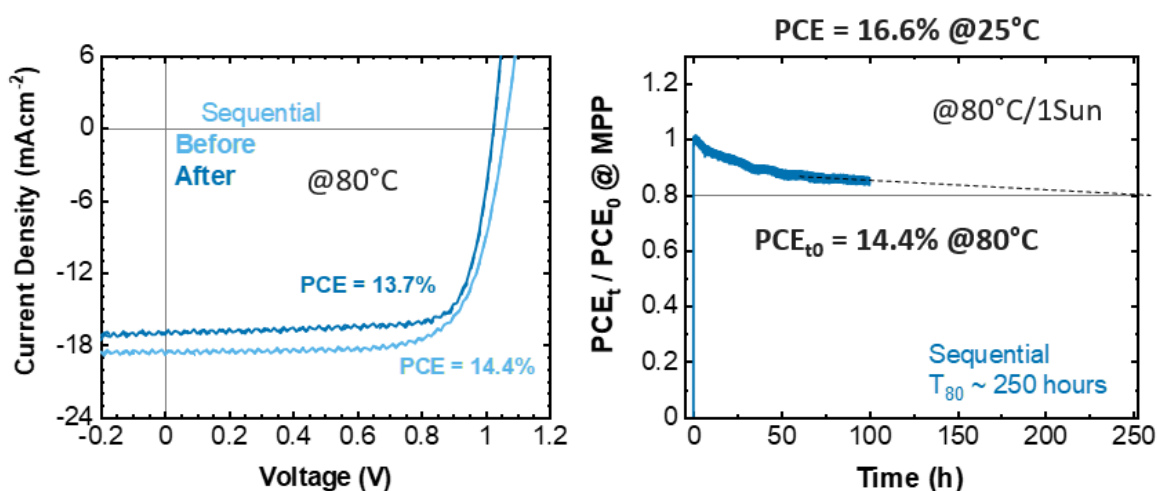


Figure 18: J-V characteristics before and after aging at 80°/1 sun (left) and MPP tracking with extrapolated T₈₀ (right) for a representative sequentially deposited ~1.68 eV perovskite solar cell.

2.2.3.2. Devices measured at UVEG

At UVEG, both semi-transparent and opaque devices were deposited via co-sublimation using a perovskite composition of Cs_{0.2}FA_{0.8}Pb(I_{0.85}Br_{0.15})₃. The full device stack consisted of ITO/MeO-2PACz/perovskite/C₆₀/SnO₂/ITO for bifacial devices, and ITO/MeO-2PACz/perovskite/C₆₀/SnO₂/Cu for the opaque ones. Figure 19 illustrates the performance evolution of several of these devices aged at 75°C under 1 sun irradiance. It is important to mention that the perovskite top cell when used in a tandem configuration with a Si-bottom cell is illuminated through the top electrode. For that reason, we prepared devices that have a semi-transparent top electrode (instead of the usually applied top metal electrode). These devices were illuminated through the transparent top electrode. All tests were conducted on encapsulated cells (using a glass-glass and UV curable epoxy resin) at 75 °C in ambient air.

In blue, the normalized PCE evolution of a transparent device—featuring an additional EDAI layer before the ETL—is shown, achieving T₈₀ of its maximum efficiency after 900 hours at 75°C under 1 sun irradiance. Two similar devices without EDAI are shown in orange and green, showing slightly poorer

results, both in stability and power efficiency. In all three cases, illumination was applied from the top, through the semi-transparent ITO electrode.

When illuminated from the bottom (red for the device with EDAI and yellow for the one without), an unexpected result was observed: at around 300 hours, both devices experienced a sudden drop in PCE to zero. As shown in Figure 20, this “sudden death” is not due to degradation of the perovskite absorber or the device stack but rather due to the patterning of the bottom ITO electrode. It can be seen that the sample appears to be “cut” exactly at the edge of the ITO electrode. We attribute this to a slightly lower distance between bottom and top electrode leading to a larger effective electric field, resulting in the sudden formation of a short-circuit at the edge of the ITO, indicating that the issue was unrelated to the absorber layer, but is related to the precise cell pattern.

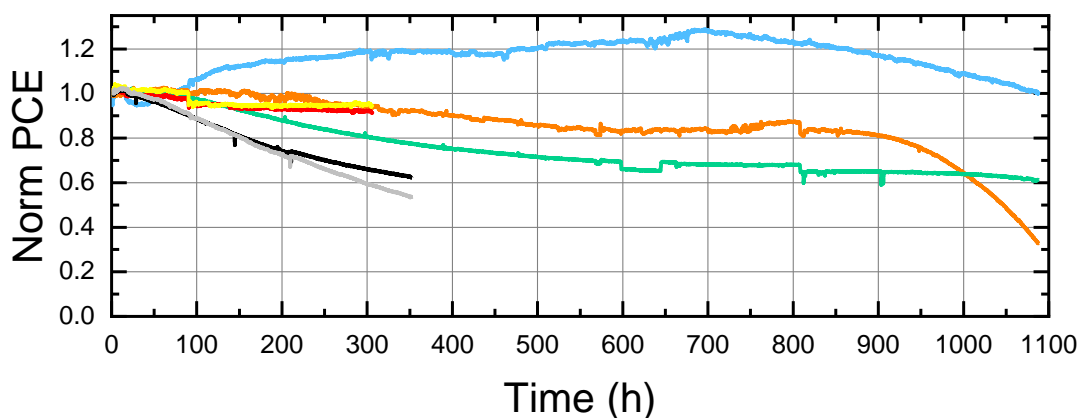


Figure 19: Evolution of the power conversion efficiency (PCE) of several devices tested at UVEG while maintaining the devices at their maximum power point and keeping them at 75 °C. The blue curve represents a semi-transparent device incorporating EDAI before the ETL, illuminated from the top. The red curve shows the same device illuminated from the bottom. A semi-transparent device without EDAI is shown in orange (top illumination) and yellow (bottom illumination). The black curve corresponds to an opaque device with EDAI and a Cu back contact, while the silver curve depicts a similar opaque device without the additional EDAI layer.

In the case of the opaque devices (black for the one using the extra EDAI layer, and silver for the one without) they degrade faster reaching 60% of the initial efficiency at 350 hours.

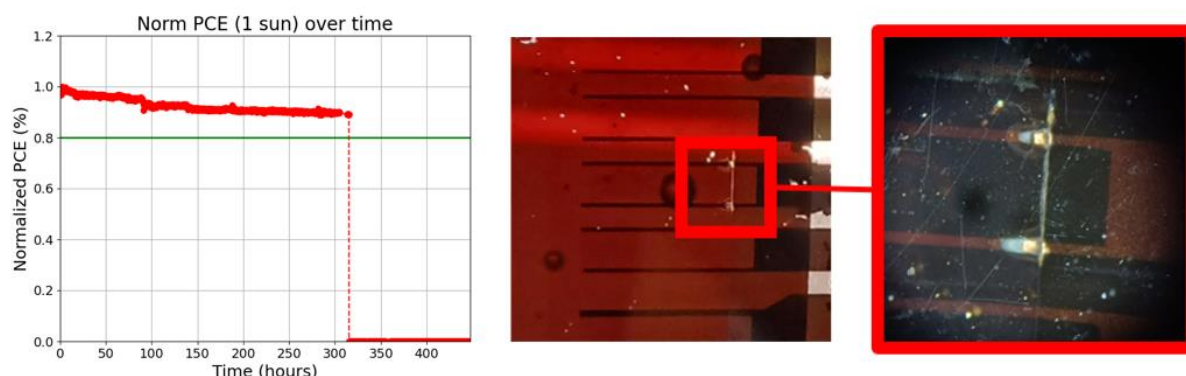


Figure 20: Closer inspection of semi-transparent devices illuminated from the bottom. The left graph displays a sudden drop in PCE occurring around 300 hours. At the center, a photograph of the affected pixel is shown, while the right panel presents a close-up of the issue: a short at the edge of the ITO, which explains the

observed performance degradation.

Linking indoor to outdoor stability

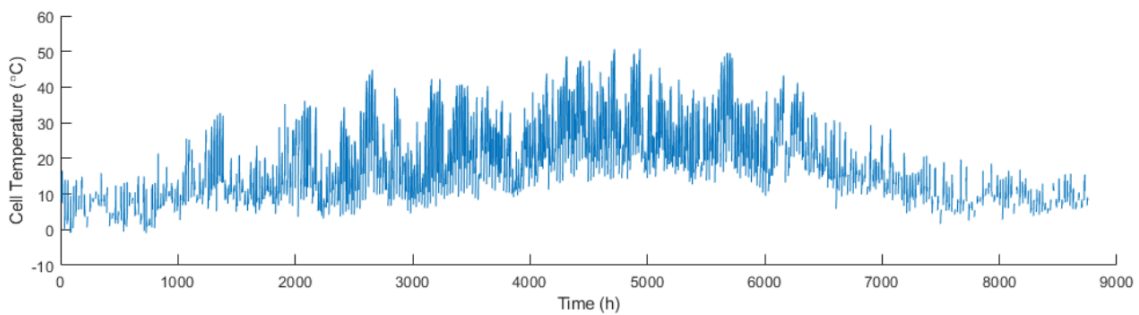
It is worth considering how the accelerated aging tests we performed indoors might translate to outdoor stability. Using data from the National Solar Radiation Database (NSRBD) from the National Renewable Energy Laboratory (NREL) in the United States, we can do just that. The indoor, temperature dependent tests give us an idea of how evaporated 1.67 eV cells degrade under illumination at different temperatures. The NSRBD contains illumination intensity, ambient temperature and windspeed data across the globe with a resolution of 4 x 4 km², from which we can estimate the cell temperature T_{cell} using the empirically derived equations derived by Albrecht et al.² and D. King³

$$T_{cell} = (0.0712W^2 - 2.441W + 29T_{amb}) \times \frac{I}{1000 W m^{-2}}$$

where T_{amb} is the ambient temperature, W is the windspeed, and I is the sunlight intensity in $W m^{-2}$. Using the NREL database, hourly cell temperature can be estimated across multiple years in any location.

We selected three locations to assess our results. Oxford (mild temperatures, low light intensity), Valencia (warm temperatures, medium light intensity) and Alice Springs (high temperatures, high light intensity). Cell temperatures from Oxford are shown in Figure 21a. Using the decay constants and activation energy curves from Figure 16, we estimate the degradation rate each hour for a typical year (average of 2019-2022) in each location. Notably, we assume that degradation is linearly correlated with light intensity, with no degradation in the dark. This is a reasonable estimate based on evidence from ref. ⁴. The predicted cell performance evolution for one of the UOXF cells for a year deployed in Oxford can be seen in Figure 21b.

a



b

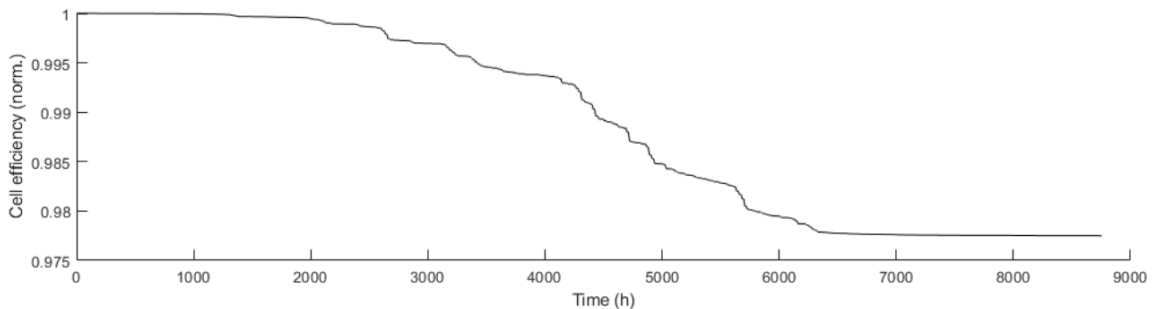


Figure 21: a) Estimated cell temperature for a perovskite solar cell over an average year (data from 2019-2022) in Oxford (U.K.). b) Simulated cell degradation over the course of an average year in Oxford (U.K.) based on activation energies and degradation rates in Figure 16, using linear light intensity decay.

Unsurprisingly, considering the strong temperature dependence of degradation at MPP, we calculate hugely different T_{80} lifetimes in each location (summary in Table 2). Using the champion device from UOXF (T_{80} lifetime of 300 hours under 75 °C), we expect a T_{80} lifetime of 14 years in Oxford, 1.85 years in Valencia and only 0.5 years in Alice Springs. Using the champion device measured under MPP from UVEG (T_{80} lifetime of 900 hours at 75 °C) we expect a T_{80} lifetime in Oxford of ~ 42 years, 5.6 years in Valencia and 1.5 years in Alice Springs. We can also estimate the lifetime for cells which would pass the T_{95} of 1000 hours at 85 °C as targeted in the NEXUS deliverable. This leads to a T_{80} lifetime of 300 years in Oxford, 45 years in Valencia and 15 years in Alice Springs. This target represents stability that would result in perovskite modules matching the stability of Si modules in many locations around the world.

Table 2: Estimation of solar cell lifetime based on the activation energy determined for the NEXUS single junction cells for different regions.

Lifetime	Description	Regional lifetime estimate (T_{80})		
		Oxford	Valencia	Alice Springs
T_{95} lifetime = 1000 hrs at 85 °C	Project goal. (@ MPP)	300 years	45 years	15 years
T_{80} lifetime = 250 hrs at 80 °C	Champion lifetime for cells assessed in KIT under MPP.	18 years	2.2 years	0.65 years
T_{80} lifetime = 300 hrs at 75 °C	Champion lifetime for cells assessed in Oxford under MPP.	14 years	1.85 years	0.5 years
T_{80} lifetime = 88 hrs at 75 °C	Median lifetime for cells assessed in Oxford under MPP (5 cells at each temperature.)	4.1 years	0.5 years	0.15 years
T_{80} lifetime = 900 hrs at 75 °C (*)	Champion lifetime for cells assessed in Valencia under MPP (of devices that passed their T_{80})	42 years	5.6 years	1.5 years

* From the three best performing UVEG cells (Figure 19) we took the second best cell for this estimation.

3. Conclusions

A strong dependence of the stability on the cell temperature was identified for the solar cells using vacuum and hybrid processed perovskites. For example, “ T_{95} stability exceeding 1000h at 85 °C and 1 sun illumination” (using MPP tracking as the bias condition) leads to a T_{80} lifetime of 300 years in Oxford (U.K.), a 50-year lifetime in Valencia (Spain) and a 15-year lifetime in Alice Springs (Australia). Considering these large differences, we suggest that though a T_{95} stability exceeding 1000h at 85 °C and 1 sun illumination is a noble target, it is overly ambitious for many global regions. Using indoor MPP tracking data under 1 sun illumination and at a cell temperature of 75 °C for the most stable of

our all-vacuum processed perovskite solar cells leads to an estimated outdoor lifetime T_{80} of 42 years for Oxford (U.K) and 5.6 years for Valencia (Spain), respectively. Although these values do need to be increased before widespread deployment can occur, they represent substantial stability and warrant delivering this technology to the other work packages in NEXUS for integration into tandem cells, modulization and outdoor stability assessments.

References

1. Domanski, K., Alharbi, E. A., Hagfeldt, A., Grätzel, M. & Tress, W. Systematic investigation of the impact of operation conditions on the degradation behaviour of perovskite solar cells. *Nature Energy* 2017 3:1 **3**, 61–67 (2018).
2. Jošt, M. *et al.* Perovskite Solar Cells go Outdoors: Field Testing and Temperature Effects on Energy Yield. *Adv Energy Mater* **10**, 2000454 (2020).
3. King, D. L. Photovoltaic module and array performance characterization methods for all system operating conditions. **394**, 347 (1997).
4. Zhu, H. *et al.* Long-term operating stability in perovskite photovoltaics. *Nature Reviews Materials* 2023 8:9 **8**, 569–586 (2023).